RADIOELEMENTS ON VESTA: AN UPDATE T. H. Prettyman[1], N. Yamashita[1], R. C. Reedy[1], H. Y. McSween[2], D. W. Mittlefehldt[3], and the Dawn Science Team, [1]Planetary Science Institute, 1700 East Fort Lowell, Suite 106, Tucson, AZ 85719, prettyman@psi.edu. [2]Earth and Planetary Sciences, University of Tennessee, Knoxville, TN 37996. [3]NASA Johnson Space Center, Houston, TX 77058.

Introduction: The main-belt asteroid 4 Vesta is the putative parent body of the howardite, eucrite, and diogenite (HED) meteorites. Because these achondrites have similar petrology, geochemistry, chronology, and O-isotope compositions, it is thought that most HEDs originated from a single parent body [1]. The connection to Vesta is supported by a close spectroscopic match between Vesta and the HEDs [2] and a credible mechanism for their delivery to Earth [3]. Studies of the HEDs show that Vesta underwent igneous differentiation, forming a Fe-rich core, ultramafic mantle, and basaltic crust [1].

Close-up observations of Vesta were made by the NASA Dawn spacecraft, which spent over a year in orbit [4]. Dawn's three payload instruments, a Visible-InfraRed (VIR) spectrometer, Framing Camera, and Gamma Ray and Neutron Detector (GRaND), acquired data on Vesta's mineralogy and chemistry. These measurements strongly support the HED-Vesta connection. Pyroxene compositions determined by VIR [5] are consistent with those of howardites, which are thought be lithified samples of Vesta's regolith. Major-element ratios measured by GRaND are consistent with the HEDs [6] and, recent geochemical mapping studies show that the compositional variability of Vesta is similar to that of the HEDs [7-10].

The abundance of radioelements can also be measured by GRaND. Compared to the Moon [11], the abundances of K, Th, and U in HEDs are very low [6, 12] and likely contributed negligibly to the thermal evolution of Vesta; however, the ratio of the moderately volatile element K to the refractory element Th is sensitive to the volatile to refractory inventory of the material from which Vesta accreted. The K/Th ratio can be compared to measurements of other solar system bodies, including the Earth, Mars, Mercury, and the Moon, providing further constraints on the distribution of volatiles in the early, inner solar system [11,13,14]. Finally, abundances of radioelements can be compared to the HEDs, providing an additional test of the HED-Vesta connection [15].

Data acquired by GRaND's bismuth germanate (BGO) gamma ray spectrometer indicated a dearth of K within Vesta's regolith, consistent with low concentrations of K in HEDs. An analysis of data acquired during the first few weeks of Dawn's low altitude mapping orbit (LAMO) indicated that K was present in quantities less than 1 mg/g [6,16]. While this is consistent with the HEDs, improved detection limits and, if possible, quantification of elements is desired. This can be achieved for two reasons: 1) the Dawn project extended LAMO to 5 months, providing a longer accumulation time; and 2) and the data reduction methods have improved and applied to a larger volume of data, enabling more accurate analyses of gamma rays near the detection limits [17].

Here we present the results of peak analyses applied to a gamma ray difference spectrum to determine the absolute abundances of K and Th. Data are compared to meteorite whole-rock compositions and other inner solar system bodies. The results, while preliminary, represent our present best estimates for these elements. Because the element signatures are near detection limits and not fully resolved, further analysis (e.g. using spectral unmixing [11]) will be required for improved accuracy and to characterize systematic errors.

Analysis. Because GRaND is a deck-mounted instrument, background contributions from the spacecraft are large. The signal from Vesta was obtained by subtracting the background measured far from Vesta (during the Approach phase) from a spectrum acquired in close proximity during LAMO (210 km altitude). The accumulation time in LAMO was about 56 days. The algorithms used to process the time series data to produce the difference spectrum are described by [15]. The spectrum provides information about globally-averaged elemental abundances.

The gamma ray spectrum contains peaks corresponding the deposition of all of the energy of a gamma ray within the BGO crystal. The area of the "full energy" peaks (counts/s) for gamma rays made by K and Th (1.461 MeV and 2.615 MeV, respectively) is proportional to the abundance of these elements in the vestan regolith. The GRaND Peak Analysis Widget (GPAW) [18] was used to fit the gamma ray spectrum in regions containing K and Th. As can be seen in Fig. 1, the peaks for these radioelements are not fully resolved; however, they are detectable as asymmetric features in the spectrum. A power-law was used to fit the underlying background continuum (baseline). The peak areas were found to be 0.055 ± 0.005 counts/s and 0.028 ± 0.008 counts/s, respectively for the 1.461 MeV (K) and 2.615 MeV (Th) gamma rays, respectively. Note that the uncertainties are statistical, and 3σ multiplied by the number of interfering peaks is given. While this is a conservative estimate for statistical uncertainty, systematic errors are not considered.
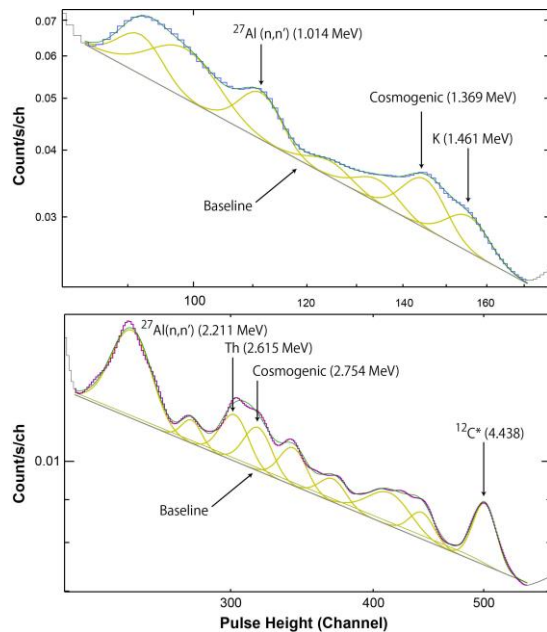
Figure 1. Peak analysis of the difference spectrum acquired by GRaND in LAMO [15]. Unresolved peaks for radioelements are detectable as asymmetric spectral features. Prominent peaks are labeled.

A simple, analytical model provides a good approximation for peak areas as a function of the abundance of radioelements. The peak area (counts/s) for a selected gamma ray is given by

$$R = \varepsilon A \frac{\Omega}{4\pi} P / \mu, \tag{1}$$

where εA is the full-energy efficiency-area product of the BGO sensor at the energy of the gamma ray [16], $\Omega/4\pi$ is the LAMO averaged fractional solid angle of Vesta [6,16], P is the specific production rate of the gamma ray of interest (gammas/g-regolith/s per µg radioelement), and μ is the mass attenuation coefficient of the regolith (cm^2/g). Gamma ray yields used to calculate P were tabulated by [19]. Application of Eq. 1 yields 1.1×10^{-4} (counts/s)/(µg/g K) at 1.461 MeV and 5.1×10^{-2} (counts/s)/(µg/g Th) at 2.615 MeV. Dividing the peak areas by these values gives 500 ± 50 µg/g K and 570 ± 150 ng/g K for Vesta's global regolith. This corresponds to a K/Th ratio of 880 ± 250.

Interpretation. The global K and Th values determined by GRaND are compared with HED meteorite whole-rock compositions in Fig. 2. The K value is well below the previously inferred detection limit of 1 mg/g, and the vestan average K and Th abundances fall within the basaltic eucrite field. [20] postulated that K-rich (but not Th-rich) lithologies might be present on Vesta's surface. One possible interpretation of the observed basaltic eucrite abundance of K is that there

are traces of these lithologies on portions of Vesta's otherwise howarditic surface; yet another interpretation – and a more plausible one at present – is that there are still systematic errors that need to be resolved.

The K/Th ratio (880 ± 250) is consistent with the mean ratio for howardites (~1200). In comparison, the K/Th ratios for Mercury, Earth, Moon, and Mars are respectively 5200 [14], 3000 [21], 360 [11], and 5500 [13,14]. The K/Th ratio measured by GRaND is consistent with Vesta's identification as the HED parent body.
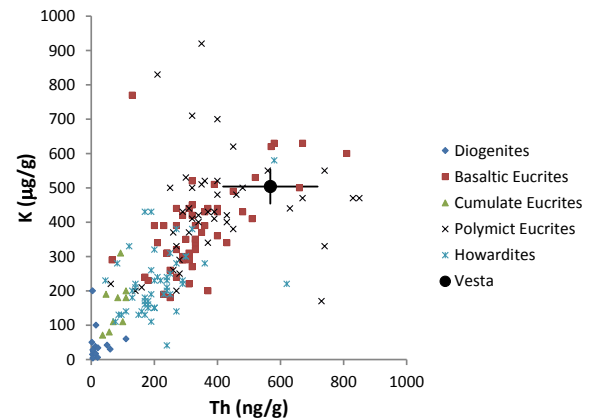

Figure 2. Scatter plot of K and Th abundances for HED meteorites tabulated by D. Mittlefehldt (Supplementary Online Materials [6]). These are compared with the average value for Vesta's surface determined by the analysis of gamma ray spectroscopy data acquired by Dawn.

References: [1] McSween H.Y. et al. (2011) *Space Sci. Rev.* 163, 141-174. [2] McCord T.B. et al. (1970) *Science*, 168, 1445-1447. [3] Binzel, R.P. and Xu S. (1993) *Science* 260, 186-191. [4] Russell C.T. et al. (2012) *Science* 336, 684-686. [5] De Sanctis M.C. et al. (2012) Science 336, 697-700. [6] Prettyman T.H. et al. (2012) *Science*, *338*, 242-246. [7] Lawrence D.J. et al. (2013) *MAPS*, *48*, 2271–2288. [8] Peplowski P.N. et al. (2013) *MAPS*, *48*, 2252–2270. [9] Prettyman T.H. et al. (2013) *MAPS*, *48*, 2211–2236. [10] Yamashita N. et al. (2013) *MAPS*, 48, 2237–2251. [11] Prettyman T.H. (2006) *J. Geophys. Res., 111*, E12007. [12] Usui T. et al. (2010) *MAPS*, 45, 1170-1190. [13] Taylor G.J. (2006) *J. Geophys. Res.*, *111*, E03S06. [14] Peplowski P.N. (2011) *Science*, *333*, 1850-1852. [15] Wasson J.T. (2013) *EPSL*, 381, 138-146. [16] McSween H.Y. et al. (2013) *MAPS*, *48*, 2090–2104. [17] Yamashita N. et al. (2014) this meeting. [18] Prettyman T.H. et al. (2011) *Space Sci. Rev*., *163*, 371-459. [19] Reedy R.C. (1978) *Proc. Lunar Planet. Sci. Conf.*, *9th*, 2961-2984. [20] Barrat J.A. et al. (2009) *MAPS*, *44*, 359-374. [21] McDonough W.F. and Sun S.S. (1995) *Chem. Geol.*, 120, 223-253.